Structural capacity of slender piles in very soft clay

Anders Jonefjäll[1*], *Åke* Andersson[2], and *Jelke* Dijkstra[1]

[1] Chalmers University of Technology, Department of Architecture and Civil Engineering, Gothenburg, Sweden
[2] University of Gothenburg, Department of Physics, Gothenburg, Sweden

1 Introduction

Deep foundations in soft soil areas in Sweden are characterised by long and slender prefabricated displacement piles with L/D in 200 – 300. The latter dimensions are governed by the need to control settlements of the pile raft, rather than the mobilisation of geotechnical bearing capacity. Furthermore, the support stiffness that can be mobilised in the soft soil surrounding the pile in the first several meters is generally low. As a result, the Swedish design guidelines for the structural capacity of these long slender piles incorporates buckling as a failure mechanism. Internationally, the buckling length is only checked in soft soils with very low strength (stiffness) and/or in case a large part of the pile is not embedded in the soil (free length in water or air) [1]. Furthermore, in liquefiable soils in areas prone to seismic loading, buckling of piles might occur (loss of support stiffness) [2].

In Sweden the critical buckling load to a fully embedded pile is conservatively designed due to the following assumptions: (1) the pile is assumed to be hinged in both ends; (2) the subgrade reaction supporting the pile is assumed to be constant with depth over a buckling length; (3) crude empirical relations are used for evaluating the subgrade reaction from the undrained shear strength, normally 50-200c_u is a first approximation.

Semi-analytical solutions to calculate the critical buckling load of a fully embedded pile have been proposed in [2-5]. The main differences stem from the assumptions made for the end-restraints, the depth dependency of any properties, and the solution procedure for the set of equations followed.

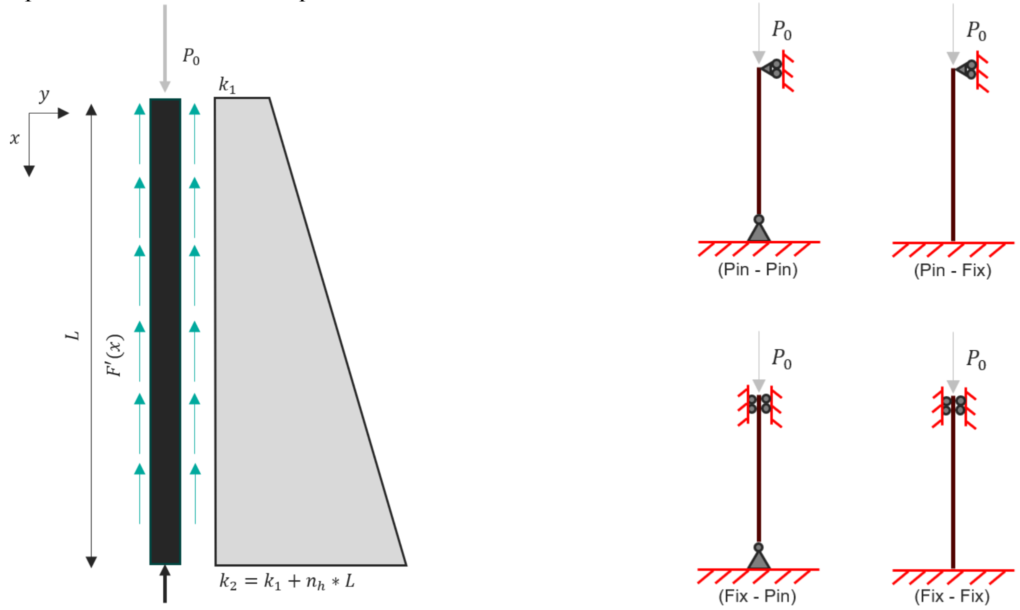

(a) (b)

Figure 1. Sketch showing the variables defining the eigenvalue problem (a) and boundary conditions used to solve the problem (b).

2 Methodology

2.1 Theory

This work numerically computes the critical axial load leading to buckling as the smallest eigenvalue P_0 of the governing equation for a pile embedded in an elastic Winkler foundation, as derived in [5]:

$$EI\frac{d^4y}{dx^4} + [P_0 - F(x)]\frac{d^2y}{dx^2} - F'(x)\frac{dy}{dx} + k(x)y = 0 \quad (1)$$

where $y = y(x)$ is the deflection of the beam as a function of position, P_0 is the axial load at the pile head (position 0), $F(x)$ is the friction integrated from 0 to x, and $k(x)$ is the stiffness of the restoring force. The above equation must be combined with self-adjoint boundary conditions (BCs) to be solvable for P_0. The eigenvalue problem is solved with a novel implementation of a finite element method (FEM) for general self-adjoint real differential eigenvalue problems.

* Corresponding author: andjone@chalmers.se

Specifically, the Ritz–Galerkin method is used with a basis of affinely transformed Irwin-Hall distributions. The weak formulation of the Ritz–Galerkin method relaxes the regularity constraint on $F(x)$ and $k(x)$, allowing for discontinuous functions (or even distributions like Dirac's delta) to be used as input to the FEM solver. This is particularly suitable for partially embedded piles where $k(x)$ is naturally discontinuous. The handling of boundary conditions is quite general, allowing any system of linear equations of the eight endpoint values $y(0)$, …, $y'''(L)$ with coefficients being polynomials of P. In particular, the FEM solver supports free end BCs characterized by $EIy''' + P\ y'$=0. In the following the original approach proposed in [5] has been adapted. The differential equation in Equation (1) is numerically approximated using the Finite Element Method.

2.2 Parametric study

Three different cases have been studied. In the first case the skin friction (shear stress mobilised along the pile) and a linear increasing subgrade reaction are considered. The second case is simplified the most, i.e. the Swedish method of calculating the critical buckling load is adopted. In the third case skin friction on the interface between the shaft of the pile and the soil is not considered, but a linear increase of subgrade reaction is. The cases are referred to as C1 to C3 respectively. For all three cases the influence of the boundary condition is studied separately, thus each case is studied with the pile head and base pinned and fixed, a schematic drawing of the assumptions and boundary conditions studied can be seen in Figure 1. The critical buckling load subsequently is used to study the impact of second order effects. For this purpose, the axial load is plotted against moment for each case and boundary condition. The second order effects are studied using a buckling curve where the pile is assumed to have some initial imperfections. The imperfection is assumed to be constant along the entire pile since this is easier to model and is considered a conservative assumption. The *p-y* curve relating the relative displacement of the pile y with the lateral resistance p is assumed to be linear elastic with a limiting resistance at yield in the soil q_k, where the limiting resistance is correlated to the undrained shear strength following [6] and [7].

For sensitive clays, that are common in Sweden, strain softening is assumed [7]. The softening is considered even though the sensitivity of remoulded soil after dissipation of the excess pore water pressures from pile installation is only very limited [8]. The sensitivities of each calculation case and boundary condition have been studied in a Sensitivity Analysis (SA). The influence of variables has been quantified using Design of Experiments (DOE) with a 2-Level Full Factorial design. The base parameters used in the SA is changed ±10% to check the influence of each parameter on the output. The base parameters and low respectively high bounds are summarised in Table 1.

Two axial loads are of interest; both the critical buckling load obtained from solving the differential equation given by [5] and the maximum axial load when buckling occurs to the pile. The SA includes both axial loads, where primary factors (main effects) are studied. The main effect of a factor is the average difference between the response when the factor is high respectively low. The main effects are normalised with the axial load calculated using the base parameters.

Table 1. Variables used for the SA.

Variable	Description	Base value	Low value	High value
L	Pile length	10m	9m	11m
EI	Pile bending stiffness	3000 kNm^2	2700 kNm^2	3300 kNm^2
O	Circumference of pile	1 m	0.9m	1.1m
α	Adhesion factor	1	0.9	1.1
c_{u_0}	Initial undrained shear strength	14 kPa	12.6 kPa	15.4 kPa
c_{u_inc}	Linear increase of undrained shear strength with depth	1.1 kPa/m	0.99 kPa/m	1.21 kPa/m
k_l	Modulus of subgrade reaction	1120 kPa	1008 kPa	1232 kPa
n_h	Linear increase of subgrade reaction with depth	88 kPa/m	79.2 kPa/m	96.8 kPa/m
y_0	Initial imperfection of pile	15 mm	13.5 mm	16.5 mm
q_k	Limiting lateral resistance of soil	126 kPa	113.4 kPa	138.6 kPa

3 Results

The following section presents some of the results from the SA conducted on both the critical buckling load and the maximum axial load. The critical buckling load depends on the calculation case and boundary conditions for the pile while the maximum axial load depends on the critical buckling load, initial imperfection and limiting lateral resistance for the soil. The main effects from the SA for C1 are shown in Figure 2. In the title of the Figures calculation case and boundary condition are annotated, followed by the critical buckling load calculated for that case with base parameters. Only C1 is shown due to limited space. Only two boundary cases are shown. For all boundary cases bending stiffness of the pile has the most influence on the result, followed by subgrade reaction. The influence of bending stiffness increases when the pile goes from pinned to fixed and the opposite applies for the subgrade reaction. The same is true for all calculation cases. In the calculation for C2, with pinned – pinned conditions, the subgrade reaction has a slightly larger impact than the bending stiffness (9.7% compared to 9.3%). The normalised effect for bending stiffness and subgrade reaction is within the same order of magnitude for all cases (±3%), i.e. for C2 pinned – pinned the effect of subgrade reaction is 9.7% while it's 8% for C3 pinned – pinned.

A change in the parameters for the skin friction has a small impact for the maximum axial load, thus C3 is shown instead since this case has fewer parameters. Buckling curves are created, in order to study the maximum axial load, using base parameters see Figure 3a. The axial and moment resistance of a 170 mm steel pile with a wall thickness of 10 mm and yield strengths if respectively 460 MPa and 550 MPa are also plotted. The computed critical buckling load, maximum axial load and the axial load at the onset of yielding of the pile material are plotted in bar charts for the 550MPa steel pile in Figure 3b. A steel pile with these dimensions represents a pile studied in the SA. The main effects from the SA on the maximum axial load is shown in Figure 4.

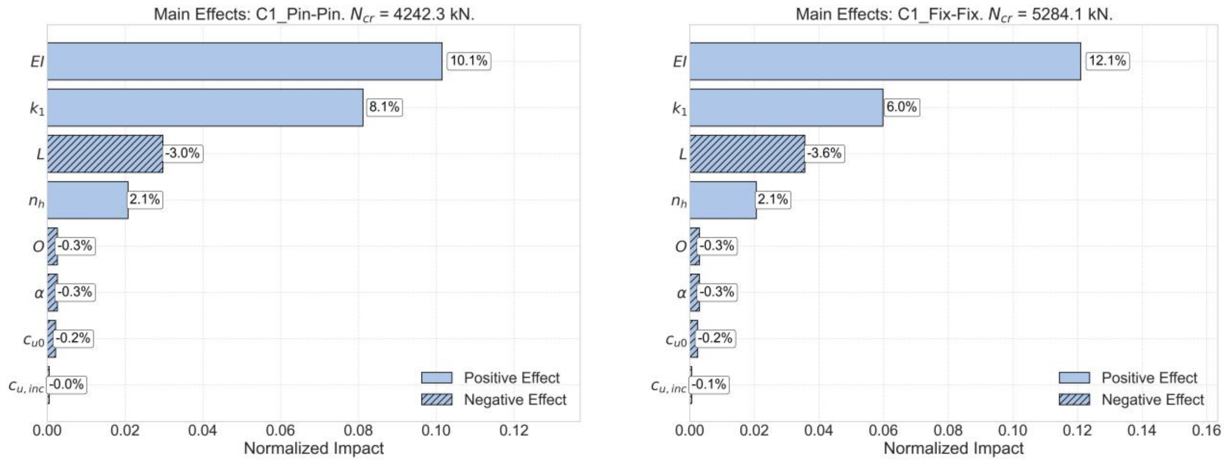

(a) (b)

Figure 2. Main effects for C1 with pin-pin (a) and fix-fix (b) boundary conditions for the critical buckling load.

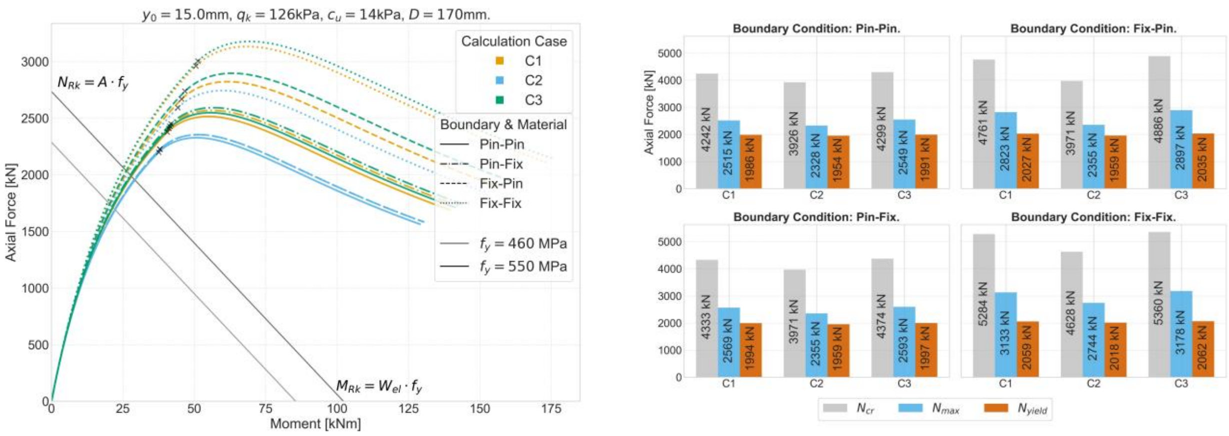

(a) (b)

Figure 3. Bucking curves (MN-curves) for each calculation using base parameters (a) with a bar chart showing the different axial loads for a 170x10mm pile with 550MPa yield strength (b).

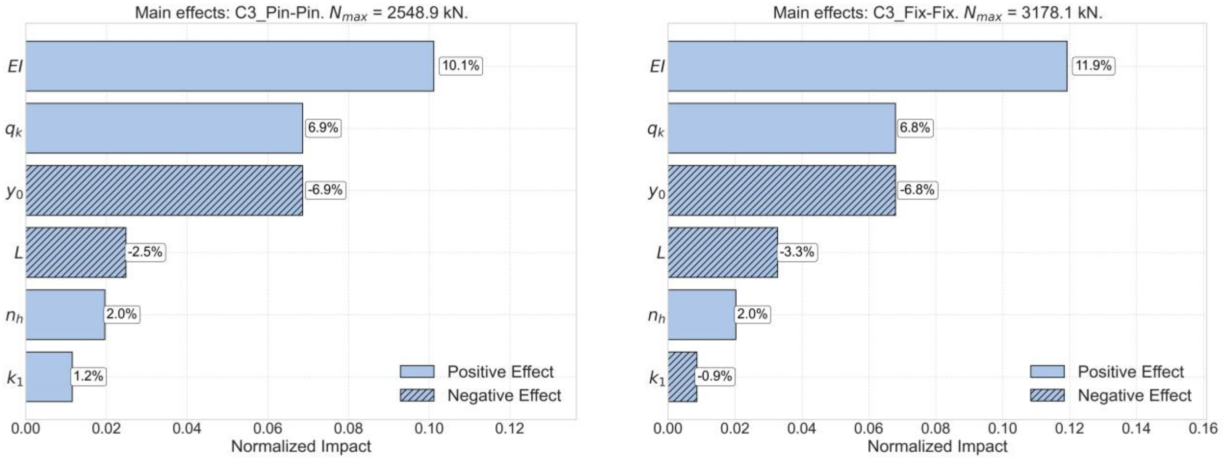

(a) (b)

Figure 4. Main effects for C3 with pin-pin (a) and fix-fix (b) boundary conditions for the critical buckling load.

4 Discussion and future work

The Ritz-Galerkin FEM used in this study is a quick, reliable and versatile tool which can give buckling loads for several different cases. The results corroborate that the Swedish design method where the subgrade reaction is assumed constant is conservative and since the subgrade reaction often is linked to the undrained shear strength of the soil, which generally is increasing with depth, this assumption is also unrealistic. The effect of this conservative assumption can be seen in Figure 3 (a) where a linear increasing subgrade reaction gives a 10% increase of maximum axial load. Buckling will occur where the horizontal stiffness of the soil is the lowest thus the boundary condition at the base will have less influence on a longer pile. The influence of a fixed pile head has significant impact on the critical buckling load for C1 and C3. For C2 the influence is a lot smaller and the difference between fixed head versus fixed base is non-existent. It becomes clear from the reference case in Figure 3 (a & b) that the limiting axial load for all cases and boundary conditions are governed by the yielding of the pile material (no buckling).

The bending stiffness of the pile has the most impact on the results, as shown in the SA for both the critical buckling load and the maximum axial load. The bending stiffness for both concrete and steel piles are well documented compared to the magnitude of the subgrade reaction, the limiting lateral resistance and the initial imperfection of the pile after installation. For the critical buckling load, the subgrade reaction is the second most influential parameter for all cases except C2 Pinned – Pinned. The limiting lateral resistance, which is the second most influential parameter, together with the initial imperfections, for the maximum axial load, is linked to the undrained shear strength of the soil. The initial imperfections of the pile after installation varies with installation method, stiffness of the surrounding soil, stiffness of the pile and the number of obstacles in the soil.

Therefore, the quantification of the subgrade reaction in the soil and the initial imperfections for an installed displacement pile is essential to get a more accurate response of the critical buckling load and the maximum axial load of the buckling curve. Yet, the expectation is that the material yielding of the pile material remains the limiting property in the majority of practical cases with long slender piles in soft soils. Finally, the financial support from Trafikverket (BIG project TRV2024/25530) and SBUF 143646 is greatly acknowledged.

References

1. K. Fleming, A. Weltman, M. Randolph and K. Elson. Piling Engineering. Taylor & Francis Group (2008). https://doi.org/10.1201/b22272
2. S. Bhattacharya, S.P.G. Madabhushi and M.D. Bolton, An alternative mechanism of pile failure in liquefiable deposits during earthquakes. Géotechnique. **54**(3), 203-213 (2004). https://doi.org/10.1680/geot.2004.54.3.203
3. M. A. Gabr, J.J. Wang, and M. Zhao, Buckling of piles with general power distribution of lateral subgrade reaction. J. Geotech. Geoenviron. Eng. **123**(2) 123-130 (1997). https://doi.org/10.1061/(ASCE)1090-0241(1997)123:2(123)
4. S. Prakash, Buckling loads of fully embedded vertical piles. Comput. Geotech. **4**(2) 61-83 (1987). https://doi.org/10.1016/0266-352X(87)90011-5
5. M. E. Heelis, M. N. Pavlović and R.P. West, The analytical prediction of the buckling loads of fully and partially embedded piles. Géotechnique. **54**(6)**,** 363-373 (2004). https://doi.org/10.1680/geot.2004.54.6.363
6. M. F. Randolph, G. T. Houlsby, The limiting pressure on a circular pile loaded laterally in cohesive soil. Géotechnique. **34**(4), 613-623 (1984). https://doi.org/10.1680/geot.1984.34.4.613
7. A. Fredriksson, Å. Bengtsson and P. E. Bengtsson, Beräkning av dimensionerade bärförmåga för slagna pålar med hänsyn till pålmaterial och omgivande jord. Pålkommissionen, Rapport 84 (1991)
8. J. Isaksson, M. Karlsson and J. Dijkstra, Modelling pile installation in soft natural clays. 10th European Conference on Numerical Methods in Geotechnical Engineering (NUMGE2023) 2023. https://doi.org/10.53243/NUMGE2023-48